Zhang *et al. Earth, Planets and Space* (2016) 68:178
DOI 10.1186/s40623-016-0555-5

Earth, Planets and Space

LETTER

Different hydraulic responses to the 2008 Wenchuan and 2011 Tohoku earthquakes in two adjacent far-field wells: the effect of shales on aquifer lithology

Yan Zhang[1*], Li-Yun Fu[1*], Yuchuan Ma[2] and Junhua Hu[1]

Abstract

Zuojiazhuang and Baodi are two adjacent wells (~50 km apart) in northern China. The large 2008 M_w 7.9 Wenchuan and 2011 M_w 9.1 Tohoku earthquakes induced different co-seismic water-level responses in these far-field (>1000 km) wells. The co-seismic water-level changes in the Zuojiazhuang well exhibited large amplitudes (~2 m), whereas those in the Baodi well were small and unclear (~0.05 m). The mechanism of the different co-seismic hydraulic responses in the two wells needs to be revealed. In this study, we used the barometric responses in different frequency domains and the phase shifts and amplitude ratios of the tidal responses (M_2 wave), together with the well logs, to explain this inconformity. Our calculations show that the co-seismic phase shifts of the M_2 wave decreased or remained unchanged in the Baodi well, which was quite different from the Zuojiazhuang well and from the commonly accepted phenomena. According to the well logs, the lithology of the Baodi well is characterized by the presence of a significant amount of shale. The low porosity/permeability of shale in the Baodi well could be the cause for the unchanged and decreased phase shifts and tiny co-seismic water-level responses. In addition, shale is one of the causes of positive phase shifts and indicates a vertical water-level flow, which may be due to a semi-confined aquifer or the complex and anisotropic fracturing of shale.

Keywords: Tidal response, Aquifer lithology, Shale, Far-field large earthquake

Introduction

Different kinds of hydrologic responses to earthquakes have been documented (Wang and Manga 2010). Many have occurred at great distances from the ruptured fault and where the associated static stress changes are relatively small (e.g., Kayen et al. 2004; Sil and Freymueller 2006; Chadha et al. 2008). Liu and Manga (2009) reported that significant water-level changes can be driven at great distances by moderate-amplitude dynamic (time-varying) stresses.

Several mechanisms have been proposed to explain these co-seismic changes in water level. Fracture clearing and increased permeability caused by earthquake-induced dynamic stress have been widely used to explain most documented far-field water-level changes (Brodsky et al. 2003; Elkhoury et al. 2006; Wang and Chia 2008; Wang and Manga 2010; Zhang et al. 2015). Overcoming capillary traps in porous channels is hypothesized to be one of the principal pore-scale mechanisms by which natural permeability is enhanced by the passage of elastic waves (Beresnev et al. 2011). Wang et al. (2009) found that groundwater flow associated with S and Love waves may generate shear stresses large enough to break up the flocs in sediment pores, thereby enhancing the permeability of aquifers. Others have theorized that the dynamic strain induced by the passage of seismic waves, most probably long-period surface waves, might be the cause

*Correspondence: evezhangyan@mail.iggcas.ac.cn; lfu@mail.iggcas.ac.cn
[1] Key Laboratory of the Earth's Deep Interior, Institute of Geology and Geophysics, Chinese Academy of Sciences, No. 19, Beitucheng Western Road, Beijing 100029, China
Full list of author information is available at the end of the article

of water-level changes in the far field (West et al. 2005; Sil and Freymueller 2006; Chadha et al. 2008 Π). In addition, the results of several laboratory experiments suggest that dynamic shaking can enhance effective permeability, especially that of fractured systems (Roberts 2005; Elkhoury et al. 2011; Candela et al. 2014). Manga et al. (2012) studied the mechanism of permeability changes using field observations and experiments and concluded that strain amplitudes as small as 10^{-6} can enhance permeability in natural systems. Other proposed but unverified mechanisms include pore pressure increases caused by a mechanism 'akin to liquefaction' (Roeloffs 1998), shaking-induced dilatancy (Bower and Heaton 1978), increased pore pressure through the seismically induced growth of bubbles (Linde et al. 1994), and the fracture of an impermeable fault (King et al. 1999).

Yan et al. (2014) studied groundwater-level changes in mainland China induced by the 2011 M_w 9.0 Tohoku earthquake. They found that earthquake-induced temporal variations in permeability might have occurred in 43% of the wells that displayed sustained water-level changes, but occurred in less than 15% of all observed wells overall. Furthermore, they found that the co-seismic phase shifts of the M_2 tidal constituent decreased for some wells, and their statistical analysis indicated no obvious significant relation between water-level changes and any other parameter (except tidal admittance). These results indicate that the processes underlying groundwater-level changes induced by distant earthquakes of great magnitude are complex.

Zuojiazhuang and Baodi are two adjacent wells (~50 km apart) in northern China. The two large far-field (>1000 km) earthquakes—the 2008 M_w 7.9 Wenchuan and 2011 M_w 9.1 Tohoku earthquakes—induced distinct co-seismic water-level responses in these two adjacent wells. The co-seismic water-level changes in the Zuojiazhuang well exhibited large amplitudes (~2 m), whereas those of the Baodi well were small (~0.05 m) and unclear. The mechanism of the different co-seismic hydraulic responses in the two wells needs to be revealed. In this study, we used the barometric responses in different frequency domains and the phase shifts and amplitude ratios of the tidal responses (M_2 wave), together with the well logs, to explain this inconformity. Our calculations show that the co-seismic phase shifts of the M_2 wave decreased or remained unchanged in the Baodi well, which was quite different from the Zuojiazhuang well and from what is commonly accepted. According to the well logs, the lithology of the Baodi well is characterized by the presence of a significant amount of shale. Due to the compact grain structure of shale, its permeability is low (approximately 10^{-4}–10^{-3} mD) (Li et al. 2013; Chen et al. 2013). With this low permeability (transmissivity), phase shifts decrease or remain unchanged even when the permeability (transmissivity) increases (Doan et al. 2006). Moreover, clogging is unlikely to be flushed out by the effect of teleseismic waves because of the compact grain structure in shale. It is therefore more difficult to enhance the permeability in the Baodi well, which has shale in its aquifer lithology, and this leads to very small co-seismic water-level changes. Meanwhile, positive phase shifts in the Baodi well indicate a vertical movement of the water level, caused either by a semi-confined aquifer or by the anisotropy and complex fracturing of shale. This needs to be clarified in the future.

Selection principles and observations

We collected data from two adjacent wells (~50 km apart) with distinct co-seismic water-level responses to the 2008 Wenchuan and 2011 Tohoku earthquakes (Fig. 1). The co-seismic water-level change in the Zuojiazhuang well exhibited large amplitudes (~2 m), whereas that in the Baodi well was small (~0.05 m) and unclear (Fig. 2). The water-level changes in this area could not have been caused by the change in static strain as it was extremely small (Kilb et al. 2002; Zhang and Huang 2011), and the co-seismic water levels in these two wells decreased regardless of whether they were located in the compressed or dilated static-strain area (Fig. 3). The mechanism of the different co-seismic hydraulic responses in the two wells needs to be revealed.

The water-level data in both wells were not influenced by pumping or other disturbances. The data were recorded over a sufficiently long time period to obtain relatively stable phase-shift information. Furthermore, although oceanic tides are known to exert an influence tens of kilometers away from the seashore (Beaumont and Berger 1975), the two wells we selected are located at distances greater than 100 km from the ocean.

Information on the two wells is shown in Table 1, including well depth, well diameter, aquifer lithology, and geological structure. The water-level recording instrument used was an LN-3A digital water-level instrument, which has an observational accuracy of ≤0.2% F.S. and a sampling rate of 1 sample/min. The resolution ratio was 1 mm. We used Mapseis software (Lu et al. 2002) to calculate the theoretical tidal strain data (solid earth tides). The tidal signal was sufficiently separate from the noise level in the two wells (Table 2).

Barometric and tidal response analysis

The well-aquifer system is composed of a well and an aquifer. The Earth tide and barometric pressure cause loading on this system by different mechanisms, contributing two input signals that are dependent on each other at certain frequencies.

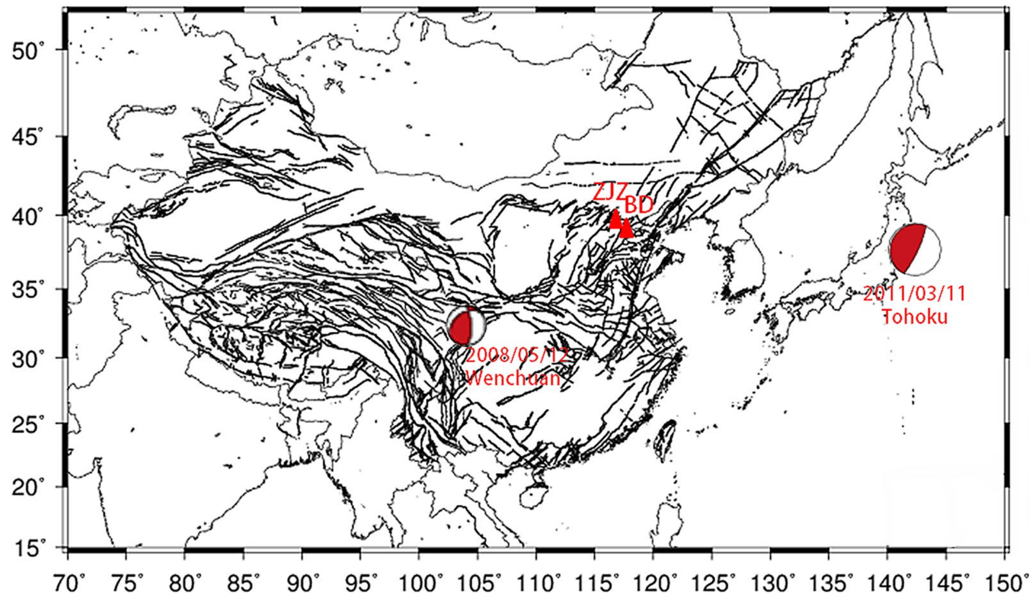

Fig. 1 Map showing the geographic locations of the Zuojiazhuang (ZJZ) well and Baodi (BD) well (*red filled triangles*), and the epicenters of the 2008 M_w 7.9 Wenchuan earthquake and the 2011 M_w 9.1 Tohoku earthquake. 'Beach ball' shows the lower hemisphere projection of the focal mechanism (from Global CMT) for each earthquake. *Black lines* indicate the location of surface faults on the Chinese mainland (Deng et al. 2006)

Ordinary coherence functions

We first calculated the ordinary coherence functions γ_{xy}^2 among the water level, barometric pressure, and Earth tide, for the Baodi and Zuojiazhuang wells. The ordinary coherence function is defined as:

$$\gamma_{xy}^2 = \frac{\left|G_{xy}(\omega)\right|^2}{G_{xx}(\omega)G_{yy}(\omega)} \tag{1}$$

where $G_{xx}(\omega)$ and $G_{yy}(\omega)$ are the power spectra of two signals and $G_{xy}(\omega)$ is the cross-spectra between them.

For the calculation, we used data from December 1, 2010, to March 10, 2011, which is continuous, stable, and not influenced by earthquakes or rainfall (Fig. 2). During the analysis of the coherence functions, the window size and step size of the Hamming window were 30 and 15 days (Lai et al. 2013b), respectively. The ordinary coherence functions of the two wells are shown in Fig. 4. We take the frequency band in which the water level is largely influenced by the Earth tide as the intermediate band (0.5–8 cpd), and the low- and high-frequency bands correspond to f < 0.5 and f > 8 cpd, respectively (Lai et al. 2013b). In the low-frequency band, the coherence functions between the water level and barometric pressure are greater than 0.9 at most frequencies, indicating that the water level is mainly responding to the barometric pressure. In the intermediate-frequency band, because the water level and the Earth tide have consistent wave components, the coherence functions between them are close to 1 at diurnal and semi-diurnal frequencies. As the barometric pressure has low energy at the frequency of the M_2 and O_1 waves, its coherence functions with water level at these two frequencies decrease obviously. In the high-frequency band, the signal-to-noise ratio in the water level is low and the barometric signals are relatively weak. The coherence functions between the water level and the barometric pressure at both wells decrease with increasing frequencies.

Barometric response analysis in the frequency domain

The transfer functions of the water-level response to barometric pressure and Earth tide for a well can be obtained by solving the following complex system of equations (Bendat and Piersol 1986; Rojstaczer 1988a, b):

$$\begin{vmatrix} BB & BT \\ TB & TT \end{vmatrix} \begin{vmatrix} HB \\ HT \end{vmatrix} = \begin{vmatrix} BW \\ TW \end{vmatrix} \tag{2}$$

where BB and TT represent the power spectra of the barometric pressure and Earth tide, respectively; BT the cross-spectra between barometric pressure and Earth tide; TB the complex conjugate of BT; BW and TW the cross-spectra between barometric pressure and water level and between Earth tide and water level, respectively; HB and HT the transfer functions of water-level response to barometric pressure and Earth tide, respectively.

From Eq. (2), we can obtain:

$$HB = \frac{TT(\omega) \times BW(\omega) - BT(\omega) \times TW(\omega)}{BB(\omega) \times TT(\omega) - BT(\omega) \times TB(\omega)} \tag{3}$$

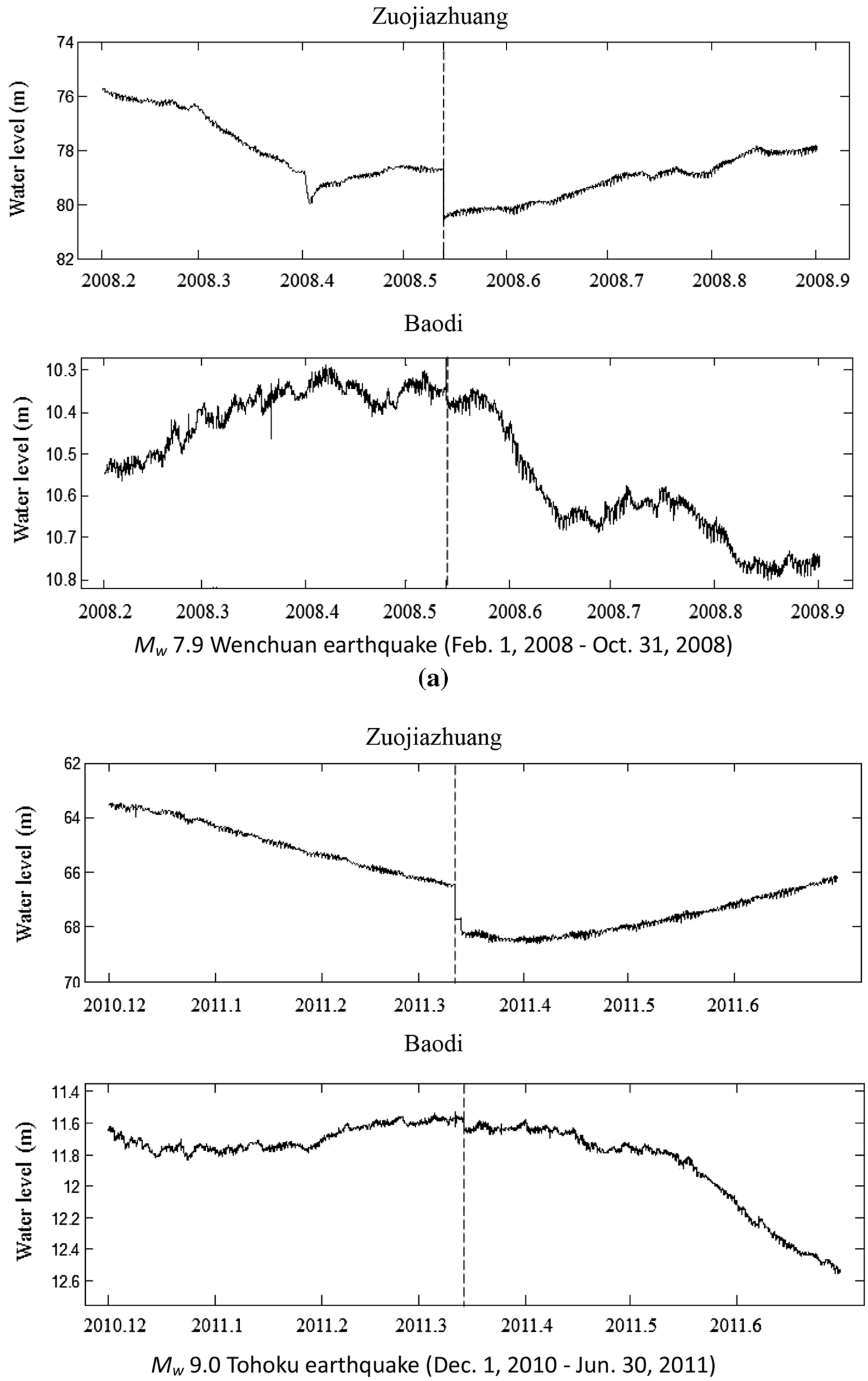

Fig. 2 Original water-level records of the two wells for the 2008 M_w 7.9 Wenchuan (**a**) and the 2011 M_w 9.0 Tohoku (**b**) earthquakes, both with resolvable tidal responses. The water level is the distance between the wellhead and the water surface inside the well. The *dotted lines* indicate the start time of the earthquake (Beijing time)

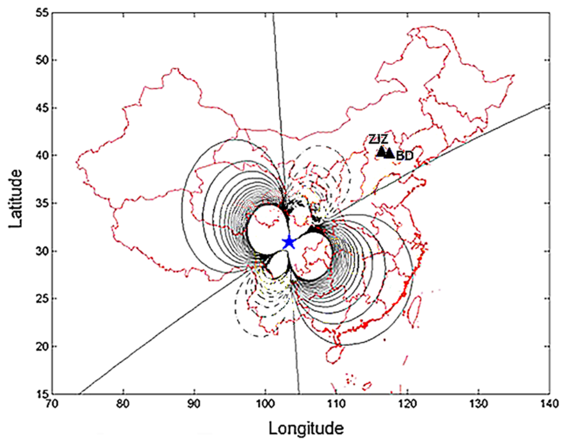

(a) Wenchuan earthquake

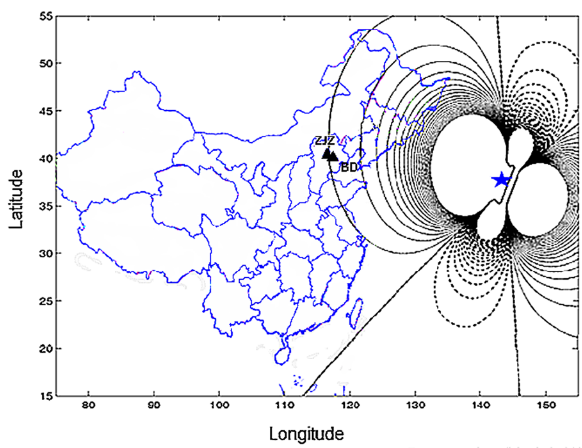

(b) Tohoku earthquake.

Fig. 3 Spatial distribution of the static volumetric strain changes for the 2008 M_w 7.9 Wenchuan (**a**) and the 2011 M_w 9.0 Tohoku (**b**) earthquakes, which were calculated using the elastic half-space dislocation model (Okada 1992). The *curved solid lines* indicate inflation, whereas the *curved dashed lines* represent compression. The *stars* are the epicenters of the earthquakes, and the *triangles* represent the stations

$$HT = \frac{BB(\omega) \times TW(\omega) - TB(\omega) \times BW(\omega)}{BB(\omega) \times TT(\omega) - BT(\omega) \times TB(\omega)} \tag{4}$$

During the analysis of the transfer functions, we used a similar data-processing method to Lai et al. (2013b). In the intermediate-frequency band, we calculated the transfer functions of the water-level response to barometric pressure and Earth tide from Eqs. (3) and (4), respectively. In the low- and high-frequency bands, the influence from the Earth tide is small, so we only calculated the transfer functions of the water-level response to barometric pressure, from Eq. (3). For the calculation, we also used the data from December 1, 2010, to March 10, 2011, which is continuous, stable, and not influenced by earthquakes or rainfall (Fig. 2).

In the low-frequency band (f < 0.5 cpd), we filtered the preprocessed water-level and barometric pressure data from 1 h to 12 days. We then calculated the power spectra and the cross-spectra with 2^{16} min (about 45.5 days) as a record, while the window size and step size of the Hamming window were ~11.4 days and 5.7 days, respectively. In the intermediate-frequency band (0.5–8 cpd), the filtered frequency band was 3 min–3 days, with 2^{15} min (about 22.8 days) as a record, and the window size and step size of the Hamming window were ~2.8 days and 1.4 days, respectively. In the high-frequency band (f > 8 cpd), the filtered frequency band was also 3 min–3 days. As the signal-to-noise ratio in the water level was low and the barometric signals were relatively weak, we stacked the data, taking 2^{14} min (about 11.4 days) as a record, with the window size and step size of the Hamming window at 8.5 and 4.3 h, respectively (Lai et al. 2013b). The barometric responses of the two wells are shown in Fig. 5.

As shown in Fig. 5, the barometric efficiencies of the Baodi and Zuojiazhuang wells decrease with increasing frequency from the intermediate- to the high-frequency band, which may be due to the wellbore storage effect (Rojstaczer 1988a). We can therefore suppose that the wellbore storage effect exists in the two wells. The phases at low frequencies are stable and close to zero and decrease with increasing frequency from the low- to the intermediate-frequency band, which also indicates that the wellbore storage effect might exist. In the intermediate-frequency band (0.5–8 cpd), the influence from the Earth tide is remarkable, and the barometric responses are therefore unstable. In the relatively high-frequency band (f > 6 cpd), the signal-to-noise ratio in the water level may be low and the barometric signals are relatively weak, and so the phases in the high-frequency range vary in a disorderly manner. As is commonly acknowledged, the phases may change much more quickly and obviously than the amplitude ratios (barometric efficiencies) after being influenced by noises or disturbances, so we neglect the phase analysis in the frequency band f > 6 cpd in these two wells.

Tidal response analysis: phase shift and amplitude ratio calculation

As analyzed by Lai et al. (2013b), the tidal responses are stable at semi-diurnal frequencies, but scatter at diurnal frequencies, which may be due to the diurnal tides being disturbed by resonances induced by the free core nutation and thermal effect (Doan et al. 2006). The tidal constituents O_1 and M_2 have large amplitudes and are less affected by the barometric effect, and are the constituents most commonly used in the interpretation of tidal analysis. However, the accuracy of the O_1 phase

Table 1 Basic information about the Zuojiazhuang and Baodi wells

Station	Well diameter/mm	Well depth/m	Geological structure	2008 M_w 7.9 Wenchuan earthquake		2011 M_w 9.1 Tohoku earthquake	
				Epicentral distance/km	Co-seismic water-level change/m	Epicentral distance/km	Co-seismic water-level change/m
Zuojiazhuang	160	2605	Next to the 'Shunyi-Qianmen-Liangxiang' fracture	1108.90	−1.917	1532.52	−1.858
Baodi	350	427.17	Intersection of Yanshan mountain alluvial plain and Jizhong hollow	1195.65	−0.046	1746.42	−0.0495

Well diameter, well depth, geological structure, epicentral distance, and co-seismic water-level change of the Zuojiazhuang and Baodi wells

is less than that of the M_2 phase, and so the most commonly analyzed phase is M_2 (Hsieh et al. 1987; Rojstaczer and Agnew 1989; Doan et al. 2006). For the tidal response analysis, we therefore focused on the M_2 phase (period = 745.2 min).

The amplitude and phase responses of water level to Earth tides have been used to monitor aquifer storativity and permeability, respectively (Hsieh et al. 1987; Elkhoury et al. 2006; Doan et al. 2006; Xue et al. 2013). In a confined system, small phase lags result from high permeability, whereas large phase lags result from low permeability. The amplitude response is primarily a measure of specific storage.

Cooper et al. (1965) demonstrated that the steady fluctuation of water level in a well occurs at the same frequency as the harmonic pressure head disturbance in the aquifer. However, the amplitude of the response is generally different from that of the disturbance, and a shift in phase is also observed. Hsieh et al. (1987) described the pressure head disturbance and water-level response as

$$h_f = h_o \exp(i\omega t) \tag{5}$$

$$x = x_0 \exp(i\omega t) \tag{6}$$

respectively, where h_f is the fluctuating pressure head in the aquifer; h_o is the complex amplitude of the pressure head fluctuation; x is the displacement of the water level from the static position; x_o is the complex amplitude of the water-level fluctuation; $i = (-1)^{1/2}$; t indicates time; $\omega = 2\pi/\tau$ is the frequency of fluctuation; τ is the period of fluctuation.

Complex notation is used in (5) and (6) to facilitate the theoretical development below. However, we are interested in only the real parts of h_f and x. The amplitude response A is defined as the ratio between the amplitude of the water-level fluctuation and that of the pressure head fluctuation. In terms of x_o and h_o, A can be expressed as

$$A = \left| x_o/h_o \right| \tag{7}$$

The phase shift is defined as

$$\eta = arg(x_o/h_o) \tag{8}$$

where arg (z) is the argument of the complex number z. The phase shift is represented by $2\pi t_p/\tau$, where t_p is the time lag between the peak water-level fluctuation and the peak pressure head fluctuation.

In the present study, we focused on the M_2 phase (period = 745.2 min). We calculated the phase lag between the water level and Earth tides using the cross-correlation method (Lai et al. 2011; Zhang et al. 2015). We calculated both the amplitude ratio and the phase lag, with a moving time window of 15 days and a running step of 3 days (Fig. 6).

According to Hsieh et al. (1987), for a homogeneous, isotropic, laterally extensive, and confined aquifer, the phase shifts between Earth tides and water level are assumed to be caused by the time required for the water to flow into and out of the well. In such a case, the water-table drainage effect is ignored, and the resulting phase shift should always be negative. An increase in phase shift (e.g., from −5° to −1°) therefore implies an increase in transmissivity or permeability (Hsieh et al. 1987; Elkhoury et al. 2006). However, positive phase shifts were observed in the Baodi well, as shown in Figs. 6 and 7, indicating that Hsieh's model is not generally applicable for describing the water-level response to Earth tides. Roeloffs (1996) presented a model in which vertical drainage to the water table can cause positive phase shifts. Figures 6 and 7 shows that the phase response values varied between positive and negative over time in the Baodi well. These phase shifts were a combination of the phase lag caused by the borehole storage effect (already proved by the barometric responses in different frequency domains) and the phase lead caused by water-table drainage.

Table 2 Amplitude and phase responses of the Zuojiazhuang and Baodi wells

Earthquake	Station	Pre-earthquake water-level amplitude response to M_2 wave/mm/nanostrain	Post-earthquake water-level amplitude response to M_2 wave/mm/nanostrain	Co-seismic change of water-level amplitude response to M_2 wave/mm/nanostrain	Background variability of water-level amplitude response to M_2 wave/mm/nanostrain	Pre-earthquake phase shift/°	Post-earthquake phase shift/°	Co-seismic phase-shift change/°	Background phase-shift variability/°
2008 M_W 7.9 Wenchuan	Zuojiazhuang	1.074	1.4748	0.4008	0.134	−29.9517	−9.6618	20.2899	8.0662
	Baodi	0.1494	0.1973	0.0479	0.0106	−5.7971	−9.1787	−3.3816	3.6399
2011 M_W 9.1 Tohoku	Zuojiazhuang	0.9453	1.4210	0.4757	0.0218	−41.5459	−4.8309	36.7150	1.3118
	Baodi	0.1747	0.2073	0.0327	0.0148	3.3816	−5.3140	−8.6957	3.7224

The pre-earthquake phase shifts and amplitude responses are single-point values obtained 15 days before the earthquake. The background phase and amplitude variability are the standard deviation of the phase shifts and amplitude responses before the earthquake for each well. The co-seismic changes were obtained by subtracting the pre-earthquake values from the single-point values after the earthquake

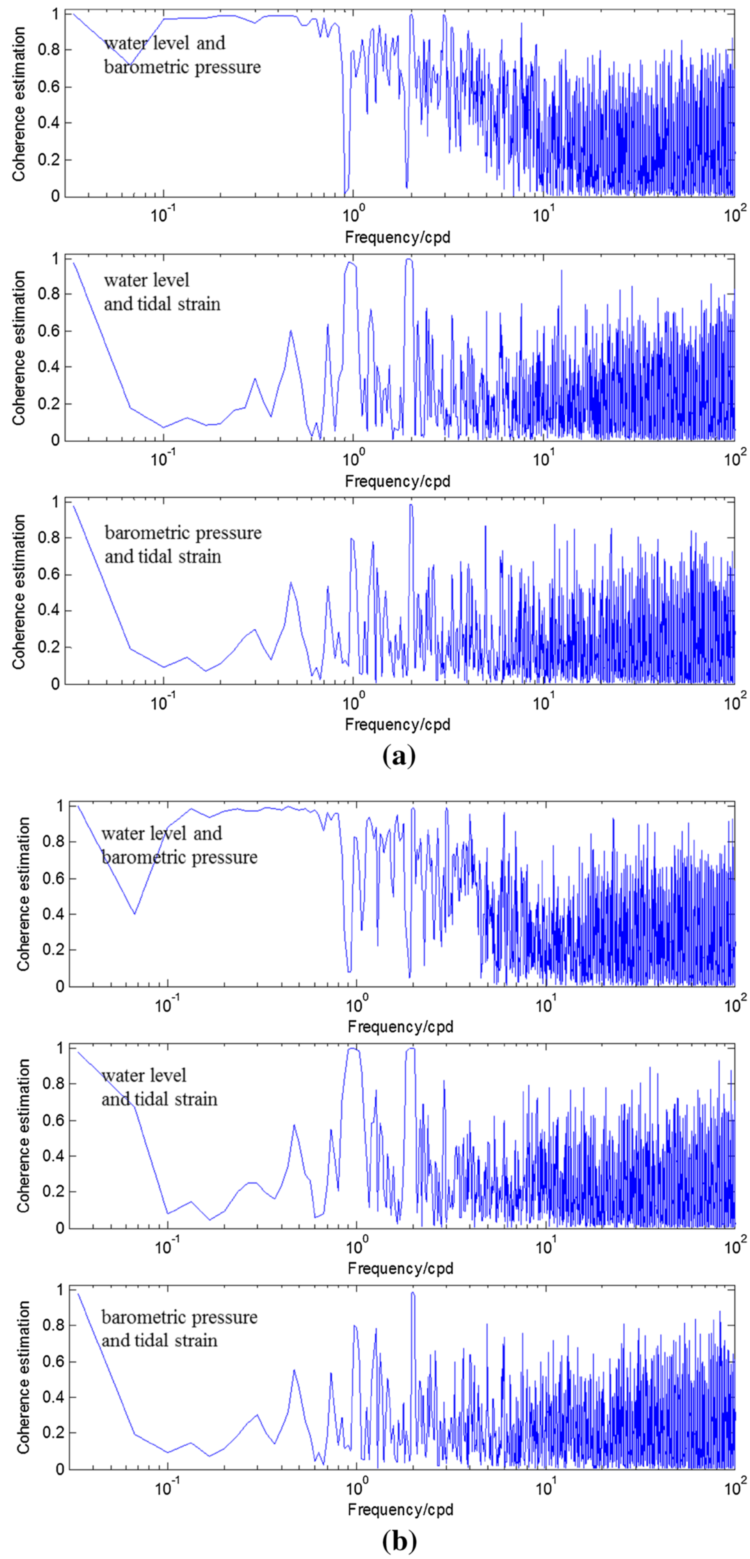

Fig. 4 Ordinary coherence functions among the water level, barometric pressure, and tidal strain for the **a** Baodi and **b** Zuojiazhuang wells

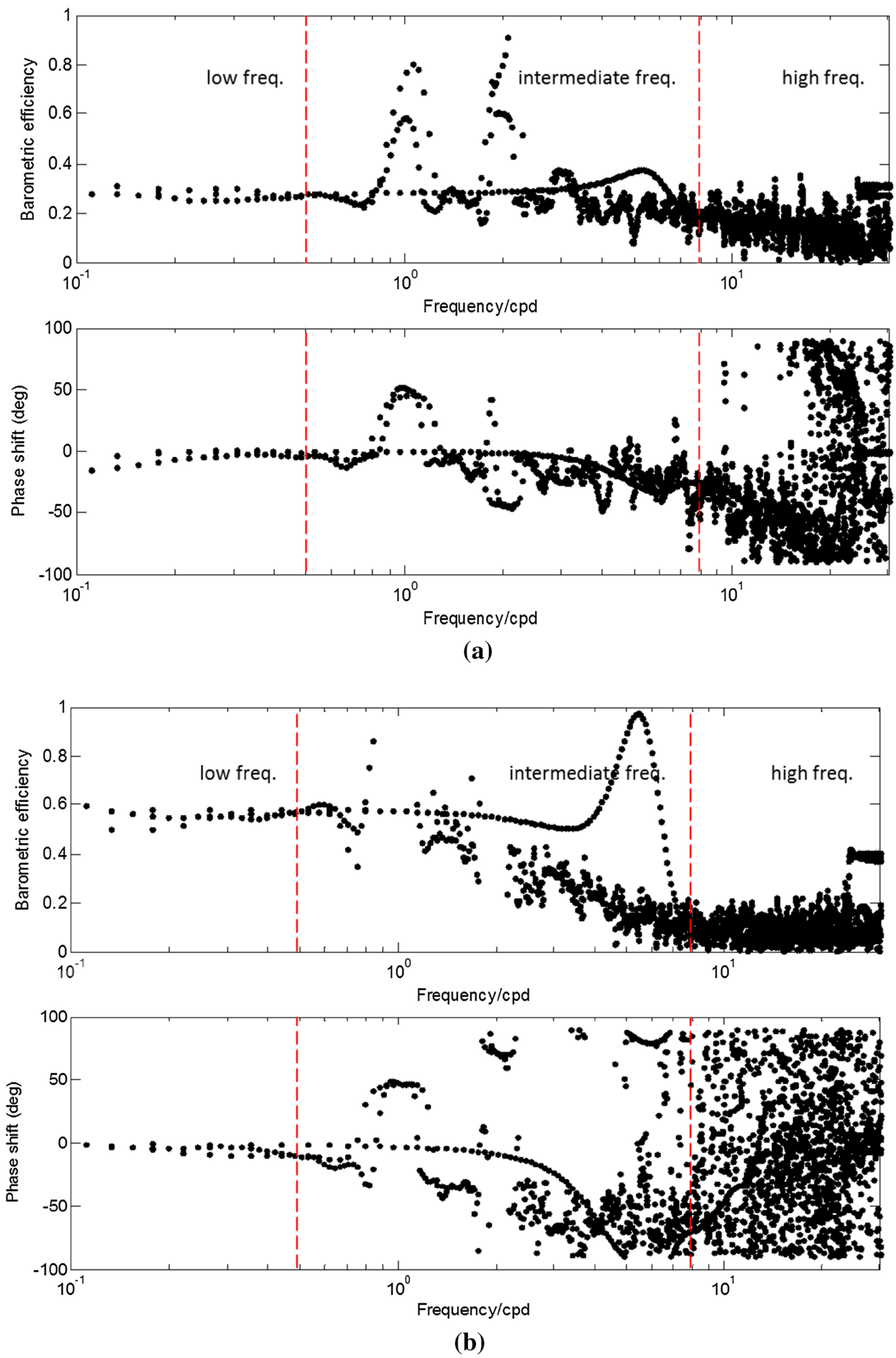

Fig. 5 Barometric efficiencies and phase shifts (*black dots*) in the low-, intermediate-, and high-frequency bands by cross-spectra estimation, for the Baodi (**a**) and Zuojiazhuang (**b**) stations. Negative phase shifts mean water level lags behind the barometric pressure

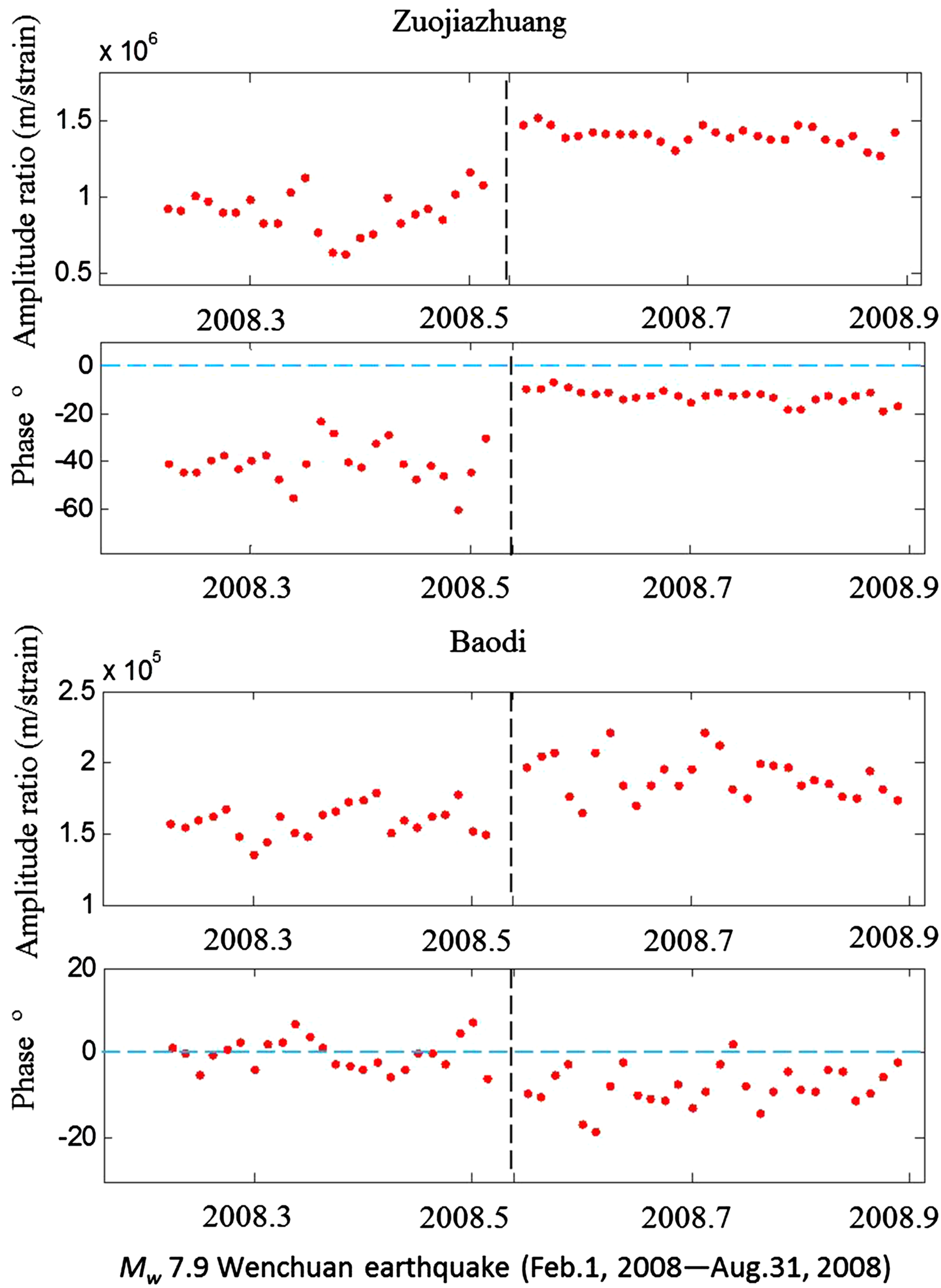

Fig. 6 Amplitude ratios and phase responses over time for the two wells at the frequency of the M_2 wave. The amplitude response is the amplitude ratio of water level over the Earth tides. The *dotted lines* show the start time of the 2008 Wenchuan earthquake (Beijing time)

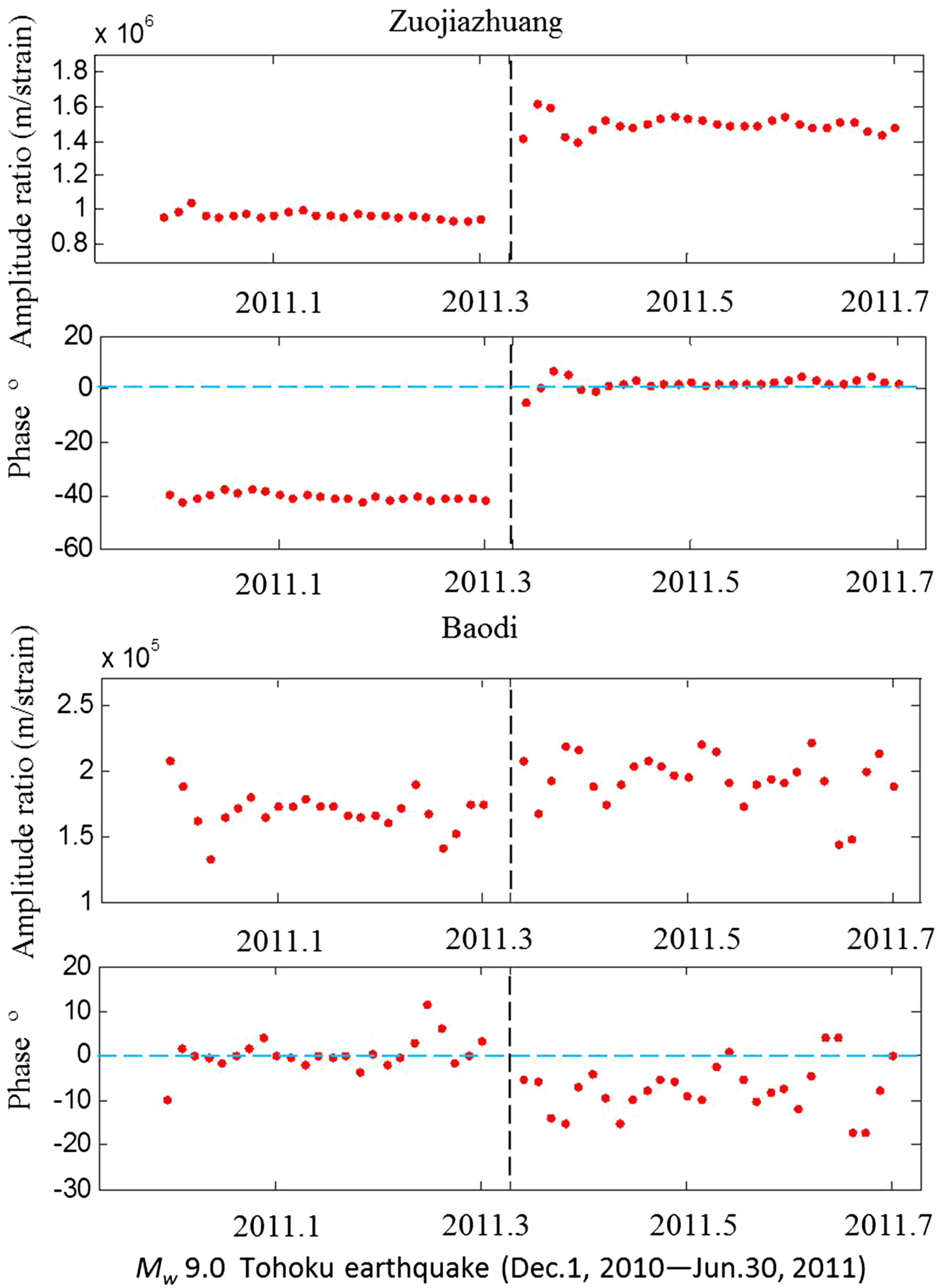

Fig. 7 Amplitude ratios and phase responses over time for the two wells at the frequency of the M_2 wave. The amplitude response is the amplitude ratio of water level over the Earth tides. The *dotted lines* show the start time of the 2011 Tohoku earthquake (Beijing time)

Lai et al. (2013a) reported that the observed phase responses can be considered a measure of permeability in both the horizontal fluid flow model (Hsieh et al. 1987) and the vertical pore-pressure diffusion model (Roeloffs 1996). Therefore, a phase-shift increase (e.g., from −10° to −5°, −5° to 5°, or 5° to 10°) implies an increase in permeability. As shown in Figs. 6, 7 and Table 2, the phase shift (permeability) in the Baodi well remained unchanged (Fig. 6) or decreased (Fig. 7) after shaking by teleseismic waves, but in the Zuojiazhuang well it increased obviously. It is necessary to compare the two wells to determine the exact mechanism of their different responses.

Aquifer lithologies

We obtained the lithologic logs of the two wells (Fig. 8) from the 'China earthquake monitoring record series' (written by the Earthquake Administration Department of each province, and various institutions in the China Earthquake Administration, and published in Beijing mainly in 2004 by Seismological Press [in Chinese]). We found shale in the aquifer lithology of the Baodi well, where there was no increase in the co-seismic phase shift. By contrast, the phase shift of the Zuojiazhuang well increased significantly after the earthquake. No obvious difference was detected in the amplitude responses of the two wells (Figs. 6 and 7).

Transmissivity (permeability) calculations

Transmissivity calculation for the Zuojiazhuang well (without shale)

The well's response depends on the flow of water through the porous medium, so it is sensitive to aquifer transmissivity and storage. Transmissivity is the rate of water transmission through a unit width of aquifer under a unit hydraulic gradient and is directly proportional to permeability. Storage is the strain change per unit imposed head and is a measure of compressibility. Additional factors of the response also include well geometry, period of oscillation, and inertial effects. The inertial effects are negligible for the long periods of the Earth tides (Cooper et al. 1965). The other two factors are independently well constrained. Thus, the amplitude A and phase η responses for the long periods of tidal oscillations are as follows (Hsieh et al. 1987):

$$A = \left(E^2 + F^2\right)^{-1/2} \tag{9}$$

$$\eta = -\tan^{-1}(F/E) \tag{10}$$

where

$$E \approx 1 - \left(\omega r_c^2/2T\right) Kei(\alpha), \quad F \approx \left(\omega r_c^2/2T\right) Ker(\alpha),\ \alpha = (\omega S/T)^{1/2} r_w \tag{11}$$

and T is the transmissivity, S is the dimensionless storage coefficient, Ker and Kei are the zero-order Kelvin functions, r_w is the radius of the well, r_c is the inner radius of the casing, and ω is the frequency of the tide.

We assume that the storage coefficient $S = 10^{-4}$, which is a typical value and the most often used for aquifers, as it is not sensitive to changes in phase and amplitude (Doan et al. 2006; Lai et al. 2011). At $r_w = 7.5$ cm and $r_c = 6.5$ cm, based on Eqs. (9), (10), and (11), we can derive the transmissivity T of the Zuojiazhuang well (Fig. 9). Within this range of transmissivity (10^{-6}–10^{-5}), the phase shifts at the frequency of the M_2 wave will increase as the permeability (transmissivity) increases (Appendix Fig. 11; Doan et al. 2006).

Permeability estimation for the Baodi well (with shale)

Given that positive phase shifts were observed in the Baodi well (which has shale in its aquifer lithology), Hsieh's model (Hsieh et al. 1987) may not be generally applicable to describe the water-level response to Earth tides for this well, and the permeability (transmissivity) should not therefore be directly calculated on the basis of Hsieh's model.

Alternatively, we could estimate the permeability (transmissivity) range for the Baodi well. The pore sizes of shaly sediments are often well below the micron scale, and most of the pores in shale are smaller than 50 nm (Josh et al. 2012). Thus, the permeability of shale is extremely low (approximately 10^{-4}–10^{-3} mD) (Li et al. 2013; Chen et al. 2013). The compact structure of the grains in shale leads to low porosity and permeability. In exploration seismology, shales are always deemed as traps (closed reservoirs). Within this low permeability (transmissivity 10^{-9}–10^{-6} m^2/s) range, phase shifts at the frequency of the M_2 wave will continue to decrease or remain unchanged rather than increase, even when the permeability (transmissivity) increases (Appendix Fig. 11; Doan et al. 2006).

Considering that the co-seismic water level changed with a very low amplitude in the Baodi well, the permeability might be harder to enhance in this well than in the Zuojiazhuang well, because of the compact structure of the shale.

Discussion

Almost all of the phases are negative in the Zuojiazhuang well, except after the Tohoku earthquake, when there are positive phases that may be caused by changes to the unconfined aquifer induced by the effect of teleseismic waves. We also calculated the continuous phase shifts over a long period during the latter half of 2011, and these phase shifts are always above zero, indicating that the properties of the aquifer medium might have been

Zuojiazhuang

Geologic age	Bottom layer depth/m	Lithology
Q	175	sandy clay, conglomerate with soft mudstone
E	566.5	conglomerate with soft mudstone
K	1210.5	sandstone, sandy conglomerate, mudstone, sandy mudstone
J	2094	andesite, andesite breccia, tuff, tuffaceous sandstone and mudstone
Z	2605	dolomite, sandy dolomite, dolomite and mudstone, argillaceous dolomite

2079 m
2600 m

Baodi

Geologic age	Bottom layer depth/m	Lithology
Q	5	surface soil
	105	sandy loam soil, fine sand, clay, silty-fine sand and medium sand
	196	silty-fine sand, fine sand, mild clay, sandy loam soil, gravel and sandy gravel
Z	254.05	shale, dolomite, argillaceous limestone, clay-stone, limestone and quartz sandstone
	320.33	shale, argillaceous limestone, dolomite, sandstone and clay-stone
	384	shale and argillaceous limestone
	427.17	argillaceous limestone, limestone and dolomitic limestone

210 m
427 m

Fig. 8 Lithologic logs of the two wells. Both records are from the seismic monitoring records of China. The *red arrows* and numbers on the *right-hand side* show the depth of the screened sections

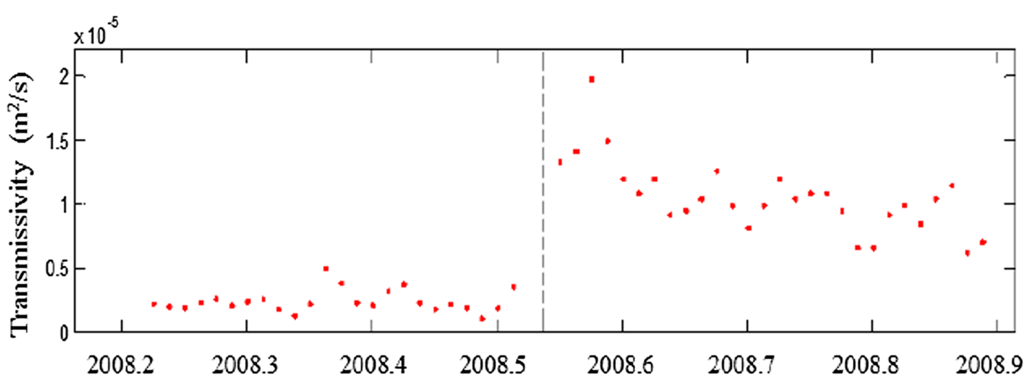

Fig. 9 Transmissivity over time from the Zuojiazhuang well before and after the 2008 Wenchuan earthquake. The *vertical dashed lines* indicate the start time of the earthquake (Beijing time)

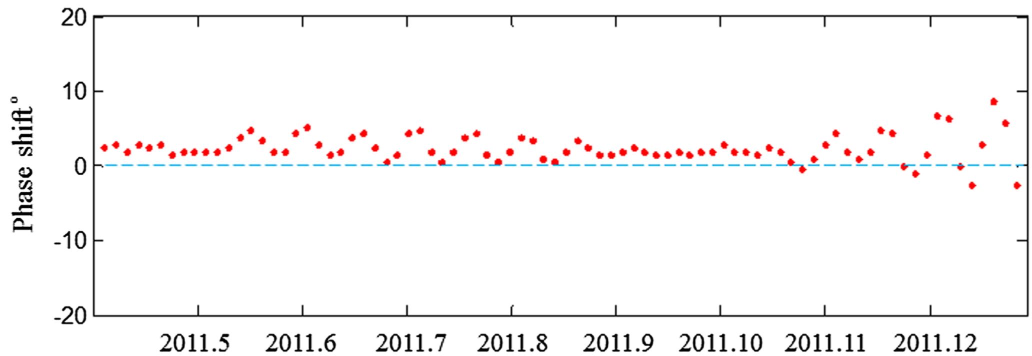

Fig. 10 Phase responses over time for the Zuojiazhuang well after the 2011 Tohoku earthquake at the frequency of the M_2 wave

changed permanently by the 2011 Tohoku earthquake (Fig. 10).

The depth ranges of the two wells (shown in Fig. 8) are different; the depth of Baodi well is much shallower than that of Zuojiazhuang well. When the aquifer is confined and Hsieh's model is completely applicable, as described by Hsieh et al. (1987) and Doan et al. (2006), the depth of the well is not related to the water-level changes. Yet when the reservoir is not confined, the flow in the confining formation is purely vertical, and the phase shifts are all positive, the water-level change is related to the depth of screening interval (Doan et al. 2006). In this study, however, there are both positive and negative phase shifts in the Baodi well, and both horizontal and vertical flow occur, and we may assume that the aquifer is semi-confined; so we may neglect the influence of the well depth on the water-level change.

Shale possesses a unique lithology with low porosity/permeability, anisotropy, and fragility. It may also contain complex fractures. Well aquifers containing shale may thus be characterized by anisotropy, and the aquifer medium may even be fractured. Therefore, homogeneity, isotropy, lateral extensivity, and aquifer confinement should not be ideally assumed in wells that feature shale in their lithology, and Hsieh's model is not necessarily applicable to wells with shale in the aquifer lithology of the screened section. The precise mechanism requires further clarification, perhaps using numerical modeling methodologies.

We hoped to elucidate the mechanism by including other large earthquakes, such as the 2012 M_w 8.6 Sumatra earthquake and the 2015 M_w 7.9 Nepal earthquake, in this study. However, because there are many disturbances and data missing from the water-level observations in the Baodi well, we had to abandon these further studies.

The permeability of wells may be relatively more difficult to enhance where shale features in their aquifer lithology, because of the compact structure of shale. This might be the reason why the co-seismic water-level changes in the Baodi well are always smaller than those of the Zuojiazhuang well. In addition, the pre-earthquake heterogeneity of the pore pressure near the well should arguably be considered. However, because the two wells are only a small distance apart, we could neglect this factor.

Conclusion

Shale has a unique lithology with low porosity/permeability, as well as anisotropy, fragility, and possibly complex fractures. It can be found in some well aquifers with specific geologic conditions. In this study, we examined the mechanism behind the different co-seismic water-level responses of two adjacent wells in the far field (>1000 km) of two large earthquakes. We used the barometric responses in different frequency domains and the phase shifts and amplitude ratios of the tidal responses (M_2 wave) to explain the uncommon co-seismic change phenomena in the Baodi well, which contains shale in the aquifer lithology of the screened section. We found that the phase shifts either continued to decrease or remained unchanged, even when the co-seismic permeability increased, perhaps due to shale's low permeability (approximately 10^{-4}–10^{-3} mD) (Li et al. 2013; Chen et al. 2013). The permeability of wells with shale in the aquifer lithology might be relatively harder to enhance because of the compact structure of shales, and this might be the reason why the co-seismic water-level changes in Baodi well are always small and unclear.

Authors' contributions

YZ and YM carried out most of the geologic investigation, data collection, and data pre-treatment. YZ finished the calculation and analysis of the phase shifts and amplitude ratios of the tidal responses and calculated the transmissivities. JH finished the co-seismic strain analysis. YZ and LYF conceived and coordinated the study and drafted the manuscript. All authors have read and approved the final manuscript.

Author details

[1] Key Laboratory of the Earth's Deep Interior, Institute of Geology and Geophysics, Chinese Academy of Sciences, No. 19, Beitucheng Western Road, Beijing 100029, China. [2] China Earthquake Networks Center, No. 5, Sanlihenanheng Avenue, Beijing 100036, China.

Acknowledgements

We thank the China Earthquake Administration for providing the data used in this study. The authors are deeply grateful to Professor Chi-yuen Wang, Xuezhong Chen, and Friedemann Wenzel for their encouragement and suggestions. We sincerely acknowledge Rui Yan, Xin Liao, Wenhui Zhang, and Guijuan Lai for their discussions on this paper. This research was supported by the Strategic Leading Science and Technology Programme (Class B) of the Chinese Academy of Sciences (Grant No. XDB10010400), the National Natural Science Foundation of China (Grant No. 41604035), and the China Postdoctoral Science Foundation (Grant Nos. 2015M570142 and 2016T90129). We gratefully appreciate the valuable suggestions proposed by the anonymous reviewers.

Competing interests

The authors declare that they have no competing interests.

Appendix

See Fig. 11.

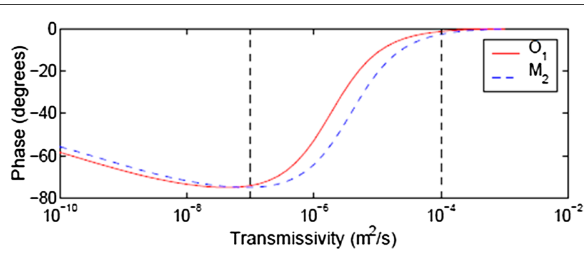

Fig. 11 Predicted amplitude and phase (negative lags) of the response of a reservoir to tides, based on Hsieh's model (Doan et al. 2006)

Received: 10 June 2016 Accepted: 27 October 2016
Published online: 11 November 2016

References

Beaumont C, Berger J (1975) An analysis of tidal strain observations from the United States of America: I. The laterally homogeneous tide. Bull Seismol Soc Am 65:1613–1629
Bendat JS, Piersol AG (1986) Random data: analysis and measurement procedures. Wiley, New York
Beresnev I, Gaul W, Vigil RD (2011) Direct pore-level observation of permeability increase in two-phase flow by shaking. Geophys Res Lett 38:231–248
Bower DR, Heaton KC (1978) Response of an aquifer near Ottawa to tidal forcing and the Alaskan earthquake of 1964. Can J Earth Sci 15:331–340
Brodsky EE, Roeloffs E, Woodcock D, Gall I, Manga M (2003) A mechanism for sustained groundwater pressure changes induced by distant earthquake. J Geophys Res 108(B8):503–518
Candela T, Brodsky EE, Marone C, Elsworth D (2014) Laboratory evidence for particle mobilization as a mechanism for permeability enhancement via dynamic stressing. Earth Planet Sci Lett 392:279–291
Chadha RK, Singh C, Shekar M (2008) Transient changes in well-water level in bore wells in western India due to the 2004 Mw 9.3 Sumatra Earthquake. Bull Seismol Soc Am 98:2553–2558
Chen Q, Liu H, Wang S, Wang LS, Liu JQ, Yang B (2013) Experimental study of the fundamental physical properties on shale in Longmaxi formation of lower silurian, Chongqing. Sci Tech Eng 13(15):796–800 **(in Chinese)**
Cooper HH, Bredhoeft JD, Papdopulos IS, Bennnett RR (1965) The response of well-aquifer systems to seismic waves. J Geophys Res 70: 3915–3926
Deng QD, Zhang PZ, Ran YK (2006) Distribution of active faults in China (1:4000000). Science Press, Beijing
Doan ML, Brodsky EE, Prioul R, Signer C (2006) Tidal analysis of borehole pressure—a tutorial. Schlumberger Research Report
Elkhoury JE, Brodsky EE, Agnew DC (2006) Seismic waves increase permeability. Nature 411:1135–1138
Elkhoury JE, Niemeijer A, Brodsky EE, Marone C (2011) Laboratory observations of permeability enhancement by fluid pressure oscillation of in situ fractured rock. J Geophys Res 116(B2): B02311/1–B02311/15
Hsieh PA, Bredehoeft JD, Farr JM (1987) Determination of aquifer transmissivity from earth tide analysis. Water Resour Res 23(10):1824–1832
Josh M, Esteban L, Piane CD, Sarout J, Dewhurst DN, Clennell MB (2012) Laboratory characterisation of shale properties. J Petrol Sci Eng 88–89(2):107–124
Kayen RE, Thompson E, Minasian D, Moss RES, Collins BD, Sitar N, Dreger D, Carver GA (2004) Geotechnical reconnaissance of the 2002 Denali Fault, Alaska, Earthquake. Earthq Spectra 20(3):639–667
Kilb D, Gomberg J, Bodin P (2002) Aftershock triggering by complete Coulomb stress changes. J Geophys Res 107(B4):2060. doi:10.1029/2001JB000202
King CY, Azuma S, Igarashi G, Ohno M, Saito H, Wakita H (1999) Earthquake-related water-level changes at 16 closely clustered wells in Tono, central Japan. J Geophys Res 104(B6):13073–13082
Lai GJ, Huang FQ, Ge HK (2011) Apparent permeability variation of underground water aquifer induced by an earthquake: a case of the Zhouzhi well and the 2008 Wenchuan earthquake. Earthq Sci 24:437–445
Lai GJ, Ge HK, Xue L, Brodsky EE, Huang FQ, Wang WW (2013a) Tidal response variation and recovery following the Wenchuan earthquake from water level data of multiple wells in the nearfield. Tectonophysics 619–620(5):115–122
Lai GJ, Ge HK, Wang WW (2013b) Transfer functions of the well-aquifer systems response to atmospheric loading and Earth tide from low to high-frequency band. J Geophys Res 118:1904–1924
Li YJ, Liu H, Zhang LH, Lu ZG, Li QR, Huang YB (2013) Lower limits of evaluation parameters for the lower Paleozoic Longmaxi shale gas in southern Sichuan Province. Sci China Ser D 56(5):710–717
Linde AT, Sacks IS, Johnston MJS, Hill DP, Bilham RG (1994) Increased pressure from rising bubbles as a mechanism for remotely triggered seismicity. Nature 371(6496):408–410

Liu WQ, Manga M (2009) Changes in permeability caused by dynamic stresses in fractured sandstone. Geophys Res Lett 36:L20307. doi:10.1029/2009GL039852
Lu YZ, Li SL, Deng ZH, Pan HW, Che S, Li YL (2002) Seismology analysis and prediction system based on GIS (Mapseis Software). Chengdu Map Press, Chengdu
Manga M, Beresnev I, Brodsky EE, Elkhoury JE, Elsworth D, Ingebritsen S, Mays DC, Wang CY (2012) Changes in permeability by transient stresses: field observations, experiments and mechanisms. Rev Geophys 50(2):81–88
Okada Y (1992) Internal deformation due to shear and tensile faults in a half-space. Bull Seismol Soc Am 82:1018–1040
Roberts PM (2005) Laboratory observations of altered porous fluid flow behavior in Berea sandstone induced by low-frequency dynamic stress stimulation. Acoust Phys 51(Supplement 1):S140–S148
Roeloffs EA (1996) Poroelastic techniques in the study of earthquakes-related hydrologic phenomena. Adv Geophys 37(1):135–195
Roeloffs EA (1998) Persistent water level changes in a well near Parkfield, California, due to local and distant earthquakes. J Geophys Res 103:869–889
Rojstaczer S (1988a) Determination of fluid flow properties from the response of water levels in wells to atmospheric loading. Water Resour Res 24(11):1927–1938
Rojstaczer S (1988b) Intermediate period response of water levels in wells to crustal strain: sensitivity and noise level. J Geophys Res 93(B11):13619–13634
Rojstaczer S, Agnew DC (1989) The influence of formation material properties on the response of water levels in wells to earth tides and atmospheric loading. J Geophys Res 941(B9):12403–12411
Sil S, Freymueller JT (2006) Well water level changes in Fairbanks, Alaska, due to the great Sumatra-Andaman earthquake. Earth Planets Space 58(2):181–184. doi:10.1186/BF03353376
Wang CY, Chia Y (2008) Mechanism of water level changes during earthquakes: near field versus intermediate field. Geophys Res Lett 35(35):86–109
Wang CY, Manga M (eds) (2010) Earthquakes and water, series: lecture notes in earth sciences. Springer Press, Berlin
Wang CY, Chia Y, Wang PL, Dreger D (2009) Role of S waves and Love waves in coseismic permeability enhancement. Geophys Res Lett 36:L09404
West M, Sanchez J, McNutt S (2005) Periodically triggered seismicity at Mount Wrangell, Alaska, after the Sumatra earthquake. Science 308:1144–1146
Xue L, Li HB, Brodsky EE, Xu ZQ, Kano Y, Wang H, Mori JJ, Si JL, Pei JL, Zhang W, Yang G, Sun ZM, Huang Y (2013) Continuous permeability measurements record healing inside the Wenchuan earthquake fault zone. Science 340(6140):1555–1559
Yan R, Woith H, Wang RJ (2014) Groundwater level changes induced by the 2011 Tohoku earthquake in China mainland. Geophys J Int 199(1):533–548
Zhang Y, Huang FQ (2011) Mechanism of different coseismic water-level changes in wells with similar epicentral distances of intermediate field. Bull Seismol Soc Am 101(4):1531–1541
Zhang Y, Fu LY, Huang FQ, Chen XZ (2015) Coseismic water-level changes in a well induced by teleseismic waves from three large earthquakes. Tectonophysics 651–652:232–241